Check for updates

Interference analysis for MIMO-OFDM based indoor visible light communication

Liwei Yang[1] [ID] **· Furong Zhu[1] · Wencong Lai[1] · Qiulian Zhang[1] · Xinlai Liu[1] · Wenjie Zhang[2]**

Abstract

Visible Light Communication (VLC) is an emerging wireless optical communication technology based on white light-emitting diode. VLC can fulfill lighting and communication needs; however, when illuminated, it produces reflections in the room, leading to a multipath effect that affects the signal quality of optical communication, thereby affecting user experience and system performance. This paper proposes a VLC system combining Multiple Input Multiple Output and Orthogonal Frequency Division Multiplexing (OFDM) using theoretical analysis. Firstly, the OFDM signal is modulated to compare the constellation distortion with the signal to noise ratio (SNR) of 25 dB and 30 dB. Experimental results show that the lower the bit error rate (BER), the more serious the distortion. Secondly, an optimal MMSE detection algorithm is proposed based on the minimum mean squared error (MMSE) signal detection algorithm and the least-squares method. Furthermore, the BER of the signal is verified by using zero forcing, MMSE and an optimized MMSE detection algorithm at the receiver of the system. The findings indicate that the optimized MMSE linear detection algorithm provides higher performance, with a BER of less than 10^{-4} at 20 dB SNR. The overall experiment results illustrate that the proposed method in this work provides the system with low BER and high reliability, improving overall system performance.

Keywords Visible light communication · MIMO · OFDM · Channel equalization · Interference

---

Furong Zhu, Wencong Lai, Qiulian Zhang, Xinlai Liu and Wenjie Zhang are contributed equally to this work.

✉ Liwei Yang
  yangliwei@cau.edu.cn

Extended author information available on the last page of the article

1 Introduction

With the rapid development of white light-emitting diode (LED) technology, visible light communication (VLC) has recently emerged as a new wireless communication technology. It uses a white LED as the light source and has good modulation characteristics [1]. VLC has the following advantages compared with conventional communication technologies: no electromagnetic interference, abundant spectrum, and high security. First, compared to the spectrum crisis that conventional WIFI and radio frequency (RF) technologies face, VLC has an unauthorized bandwidth of 400 THz. Second, the VLC uses visible light as a carrier frequency, avoiding interference with other electronic devices. Third, the VLC is easy to implement, requiring only LED lighting and micro-controllers. Fourth, the VLC link can easily set up high-speed communication links above 10 Gb/s. Therefore, it is predicted that in the future, VLC will become one of the essential means of communication and also one of the most frequently utilized bandwidths [2, 3].

VLC has attracted much attention from both domestic and foreign experts. A VLC system with independent uplink and downlink that can realize the interference-free transmission of uplink and downlink data and then complete the bidirectional communication has been proposed in Ref. [4]. A visible light orthogonal frequency division multiplexing (OFDM) system for channel estimation and interference processing has been developed in some studies. By combining precoding with iterative clipping filtering technology and using FFT/IFFT clipping filtering for improvement, a better bit error rate (BER) performance has been obtained in Ref. [5]. The Ref. [6] has been proposed that an optical cellular configuration model for the problem of lighting distribution leads to communication in the central blind area of the room. This model provides uniformly distributed lighting and optimizes the field of view in the communication system to improve the system performance. It has been identified that an improved channel estimation algorithm based on cyclic prefix (CP) for multiple-input multiple-output (MIMO)-OFDM systems can suppress the noise generated during channel transmission in Ref. [7]. However, the optimization effect did not improve significantly compared to traditional algorithms. The Ref. [8] has discussed the denoising problem of VLC systems based on MIMO-OFDM. Compared with the conventional VLC system, the proposed scheme has a 10dB improvement in the system gain. However, there is no further research on channel equalization techniques in this study. Aiming at the problems of inter-channel interference (ICI) and inter-symbol interference (ISI), the previous symbol's channel slope eliminates the interference received by the current character in Ref. [9]. In Ref. [10], the system performance is improved by increasing the diversity gain in the MIMO channel.

However, there are still some critical issues for the VLC system to resolve. Due to the inevitable randomness of the free space channel and the complexity of the VLC system structure, the indoor VLC system is subject to different kinds and degrees of interference during data transmission. These distractions may cause transmission signals to produce error codes, affecting the quality of

system communications [11]. If the signal interference is so severe that the signal cannot be transmitted, or even if the communication process is interrupted, the user experience will be seriously affected. Furthermore, much research has been conducted on single VLC and MIMO-OFDM systems [12, 13]. Therefore, less research has explored the combined benefits. Given the above problems, the main contributions of our work are:

1. It proposes a VLC system based on MIMO-OFDM, where the OFDM technology is employed to modulate the signal during transmission in order to eliminate various interferences during communication. The MIMO technology is employed for data transmission to increase system capacity. The signal is modulated using quadrature phase-shift keying (QPSK) technology, and a guard interval is introduced between the signals. The CP and cyclic suffix (CS) in the guard interval can ensure that the subcarriers are orthogonal to each other and reduce the interference of multipath effects.
2. It proposes an optimized minimum mean square error (MMSE) algorithm based on least-squares algorithm. The traditional channel detection algorithm and the optimized channel detection algorithm are used to detect the signal at the receiver under different interference cancellation conditions and compare BER performance of different algorithms.

The rest of the paper is structured as follows: the second section is the related work, the third section introduces the principle of MIMO technology and OFDM technology and constructs a new VLC-based MIMO-OFDM system, the fourth section is the simulation experiment and the analysis of the experimental results, and the conclusion is drawn in the last section.

2 Related work

Furthermore, several researchers have investigated VLC interference. In Ref. [14], a zero-forcing (ZF) equalizer with successive interface cancellation (ZF-SIC) and a MMSE equalization with subsequent interface cancellation (MMSE-SIC) have been utilized to enhance the BER performance in the context of VLC. The performance of MMSE-SIC is improved by 3dB SNR compared to ZF-SIC to achieve the same BER of 10^{-3}. A model to enhance the performance of MIMO VLC has been provided in Ref. [15], which simultaneously employs the ZF-SIC and MMSE-SIC equalizers in Ref. [14]. Even in higher-order MIMO, MMSE-SIC offers better performance in this system. Ref. [16] proposes an non-orthogonal multiple access (ISIC) receiver, which significantly reduces the BER of non-orthogonal multiple access (NOHO)-OFDM considerably. The ISIC algorithm can converge in a single iteration for any NP-hard task.

Table 1 illustrates the findings of comparing the different channel interference elimination techniques described in the above research. The method proposed in this work is listed in the table.

Table 1 Summary of different channel interference cancellation methods

Issues	Methods	T_x & R_x	Advantages	Limitations	Performance	BER
NOMA- MIMO- VLC [14]	ZF-SIC MMSE-SIC	2*2	1.NOMA improves spectral efficiency. 2.Comparing the BER of ZF-SIC and MMSE-SIC	The achievable rate, fairness, and outage probability of this system based on equalization techniques are not considered	MMSE-SIC improves BER by 3 dB of SNR	$<10^{-3}$
MIMO- VLC [15]	MMSE-SIC	2*2	MMSE-SIC gives better performance even for higher order MIMO	It is more complicated to implement, and the algorithm complexity is high	MMSE-SIC equalizer outperforms other equalizers and algorithms	$<10^{-2}$
NOMA- OFDM- VLC [16]	ISIC	not available	1.Subcarriers can be flexibly and nonorthogonally allocated. 2. ISIC scheme can be basically converged after one iteration	The bandwidth is lower, resulting in a lower SNR	The proposed scheme is superior than conventional scheme in terms of BER performance and data rate	$<10^{-3}$
MIMO- OFDM- VLC (this work)	Optimized MMSE	2*2	The complexity of the detection algorithm is low.	The BER is not ideal when the SNR is low.	Optimized MMSE algorithm has more over gain than traditional MMSE algorithm.	$<10^{-4}$

3 System model

3.1 MIMO technology

MIMO technology has multiple independent channels between the transmitter and the receiver. These independent channels eliminate the correlation of signals between antennas, hence enhancing signal link performance and improving data throughput. The most common MIMO techniques in VLC systems include diversity technology and space division multiplexing (SDM) technology [17–19]. However, diversity technology suggests the transmission of redundant data, which is inefficient, whereas SDM technology pursues a significantly increased transmission rate, which is unreliable. Therefore, suitable solutions are needed according to different situations and practical applications [20].

The principle of MIMO is illustrated in Fig. 1. At the system's transmitter, the serial electrical signal becomes several parallel signals after modulation and data processing. Parallel signals are processed by the transmission module and become optical signals emitted by LED terminals. Optical signals are transmitted to the receiver through the MIMO matrix channel and are processed by photoelectric detector (PD) to obtain multiple received signals [21, 22]. Finally, sampling detection and demodulation recovered the original transmission signal x'. The formula for the receive signal y is expressed in Eq. (1):

$$y = \varphi H(x) + n \tag{1}$$

$$\varphi = \frac{P}{S} \times 100\% \tag{2}$$

Where x is the serial signal of the transmitter, H is the channel matrix, and φ is the photoelectric conversion efficiency, which indicates how much of the optical signal received by the receiving module from PD can be converted into an electrical signal, and n is the added noise in the signal. P is the transmit power of the signal at the transmitter, and S is the illumination area.
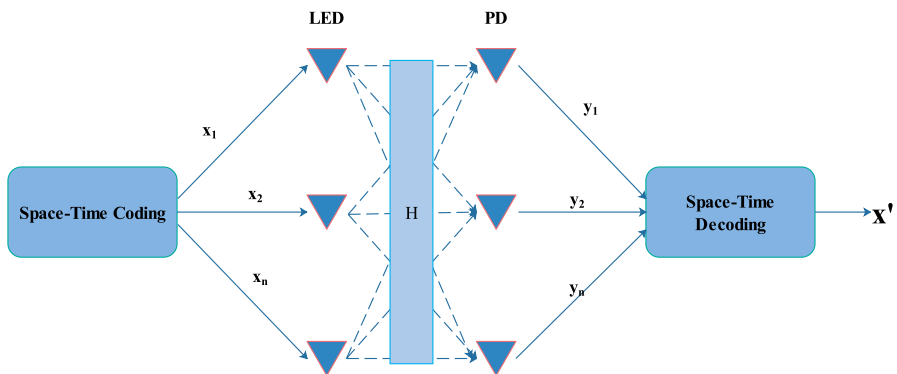

Fig. 1 MIMO schematic diagram

3.2 OFDM technology

OFDM is a method for continuously transmitting multiple data streams on multiple subcarriers in a parallel mode. It can be described as a modulation or multiplexing technique. The following are its advantages [23, 24]:

(1) Low complexity;
(2) High spectrum utilization;
(3) Strong resistance to decline;
(4) Easy integration with other systems;
(5) Resistance to narrowband interference.

   VLC systems can use OFDM technology. The implementation of OFDM in a VLC system is described and analyzed in Ref. [25], which highlights how conventional OFDM fits within the limitations of an optical system and describes the implementation of OFDM in a VLC system. OFDM modulation and demodulation are depicted in Fig. 2. It is necessary to maintain orthogonal frequency between subcarrier channels in OFDM to eliminate carrier interference effectively. Multipath delay results in pulse broadening, overlapping between adjacent signals, and ISI. In addition, the OFDM system requires high orthogonality of symbols, and however, if the orthogonality between signals is broken, it will affect the demodulation of the receiving signal, known as ICI. Furthermore, string conversion and protection interval are two approaches commonly employed to eliminate multipath interference.

3.3 MIMO-OFDM based VLC system

Figure 3 depicts a simple indoor multi-cell VLC system. In the system, an external signal input to each LED array's communication access point (AP) can be used for bidirectional transmission between users and devices. The architecture of the system has four levels: the first layer is for intelligent device nodes that can perceive LED visible light signals; the second layer is for clusters of LED optical communication nodes based on factors such as the actual transmission of light; the third layer defines clustered communication protocols in different communication regions to
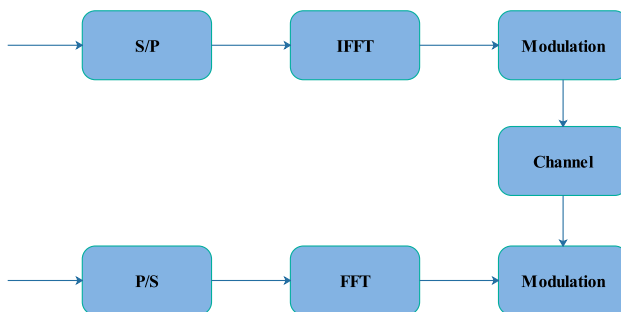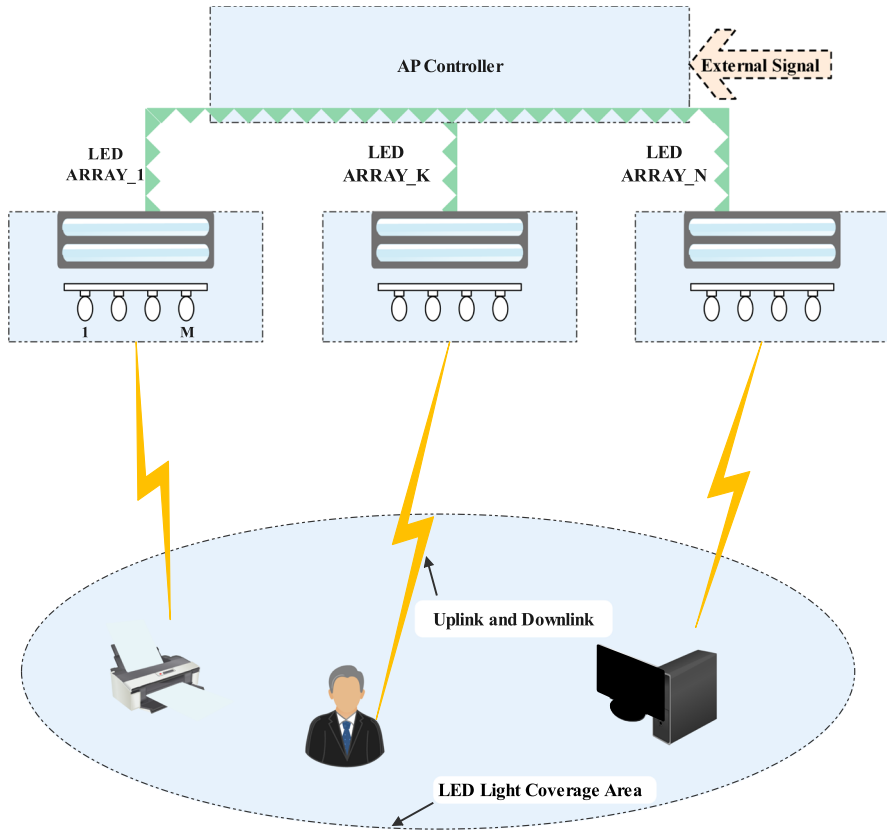

Fig. 2 Modulation and demodulation of OFDM

Fig. 3 Indoor multi-cell VLC system model

achieve inter-cluster communication, and the last layer is for optical communication across regions to enable LED optical communication nodes to interact with information on the internet [26–28].

The signal transmission process modulates the original signal into a drive circuit of LEDs, which therefore transmits the electrical signal in the form of an optical signal carrying the transmission information. Employing coding modulation at the transmitter is intended to achieve high-speed transmission with a narrow bandwidth. In areas covered with LEDs, transmission-carrying light signals are transmitted as visible light. The information-carrying light signals converge at the receiver on the PD. PD converts the light signal back into an electrical signal, which is amplified, decoded, and demodulated in the amplified plastic circuit to provide the output signal.

In order to resist the severe frequency selective fading that occurs when the transmitted signal in the VLC system is transmitted in the wireless channel, ensure the communication quality, and improve the reliability of the VLC system, the MIMO technology with strong anti-channel fading characteristics and the OFDM

technology with anti-ISI characteristics are combined to form a new MIMO-OFDM system based on VLC. Figure 4a and b describe the system block diagram of the transmitter and the receiver of the MIMO-OFDM system, respectively. The transmitted signal is subjected to space-time encoding in the MIMO encoder, then modulated by OFDM, and finally sent out by an antenna array composed of multiple antennas. The system consists of N_T LED transmitters and N_R PD receivers.

In the MIMO-OFDM system, the channel state information (CSI) plays a decisive role in the detection and recovery of the received signal in the process of coherent demodulation. Therefore, the MIMO-OFDM system needs a variety of techniques to be used and combined in its operation. Nevertheless, it comprises several methods [29–31]:

(1) Achieving a predetermined gain;
(2) SDM techniques for enhancing spatial gain;
(3) Channel estimation techniques for evaluating CSI;
(4) Signal detection techniques for MIMO channel equalization;
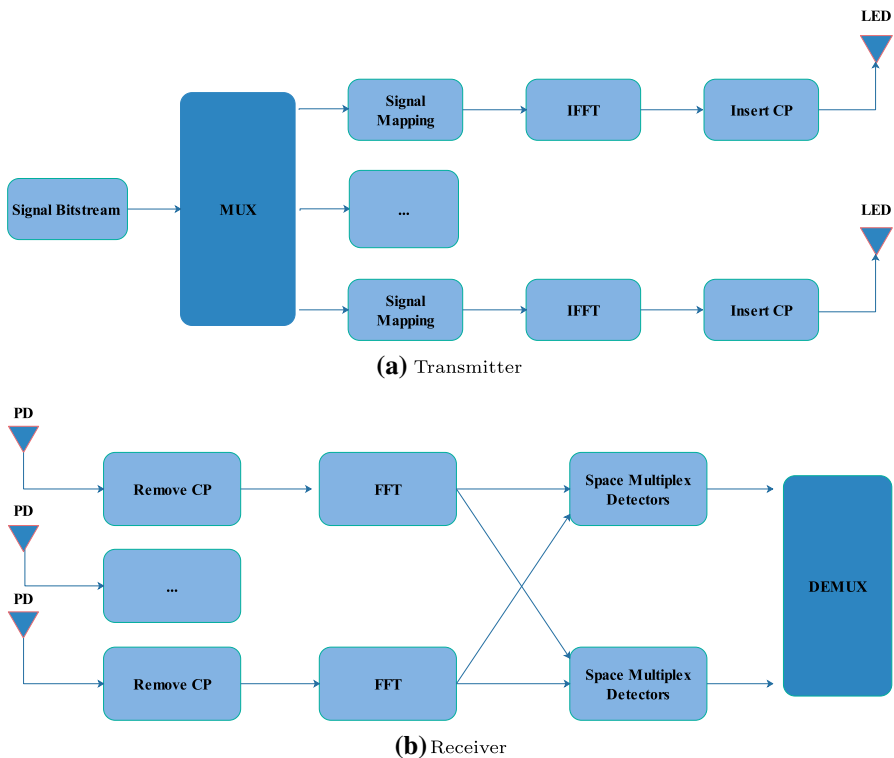(5) Methods for adding protection intervals to OFDM symbols to eliminate multipath interference.

(a) Transmitter

(b) Receiver

Fig. 4 MIMO-OFDM based VLC system block diagram

After the system modulation, some data streams become OFDM symbols, reducing the influence of multipath fading channels by extending the cycle of OFDM symbols. However, the attenuated impact still destroys the orthogonality between subcarriers in OFDM communication systems, affects the standard transmission of signals in channels, and reduces the reliability of communication systems. Therefore, a protection interval is added to the OFDM symbol during transmission. The number of waveform cycles included in the delayed copy of the FFT cycle is an integer, thus ensuring no crosstalk between codes. The length of the protective interval between inserts is not a fixed value but must be greater than the maximum delay extension of the channel. The addition of CP and CS in the protective interval also ensures orthogonality between subcarriers. The choice of CP length is closely related to the delay extension of the wireless channel and the cell diameter.

$$C = \max I(x;y) \tag{3}$$

$$I(x;y) = H(y) - H(y|x) \tag{4}$$

$$y = \sqrt{\frac{E_x}{N}} H(x) + z \tag{5}$$

Where C is the channel capacity, x is the random vector at the transmitter, y is the random vector at the receiver. $I(x; y)$ is the mutual energy of x and y, $H(y)$ is the differential entropy of y, $H(y|x)$ is the differential entropy of y given that the event x has occurred. y is the receiving signal, z is the additive white noise of the receiving antenna, and E_x is the energy of the transmitting signal.

$$H(y|z) = H(z) \tag{6}$$

$$
\begin{aligned}
R_{yy} &= E\{yy^H\} \\
&= E\{(\sqrt{\frac{E_x}{N}} H(x) + z)(\sqrt{\frac{E_x}{N}} x^H H^H + z^H)\} \\
&= E\{(\sqrt{\frac{E_x}{N}} H(x) x^H H^H + zz^H)\} \\
&= \frac{E_x}{N} H R_{xx} H^H + N_0 I_N
\end{aligned}
\tag{7}
$$

$$H(y) = \log_2\{\det(\pi e R_{yy})\} \tag{8}$$

$$H(z) = \log_2\{\det(\pi e N_0 I_N)\} \tag{9}$$

Where R_{yy} is the self-covariance matrix of y and N_0 is the power spectrum density of z. H is for channel matrix and $(.)^H$ is for transposition operation. Equation (6) can be obtained from the independence of x and z. $H(z)$ is the differential entropy of z. When $H(z)$ is constant and y is subject to the symmetric complex Gaussian

distribution of a zero-mean cycle, $H(y)$ reaches its maximum value, which is the maximum mutual energy.

Equation (10), the maximum channel capacity, can be obtained by employing Eqs. (3–9):

$$C = \max I(x;y)$$
$$= \log_2\{\det(I_N + \sqrt{\frac{E_x}{N}}HR_{xx}H^H)\} \tag{10}$$

The Vertical-BLAST (V-BLAST) is used to implement spatial partitions in the MIMO-OFDM model based on the detection scheme adopted by the receiver after receiving the signal. Different detection systems correlate to various algorithms, and the BER varies based on the detection scheme. The ZF, MMSE, and optimized MMSE algorithms are used to detect the signal at the receiving end of the V-BLAST structure. The channel equalization algorithm is based on the following assumptions:

(1) Half-wavelength antenna spacing;
(2) Rayleigh fading channel;
(3) Channel equalization with perfect channel estimation at the receiver.

3.3.1 ZF algorithm

The criterion of ZF detection algorithm is to make the interference between users and the data flow within users nearly zero.

$$y = Hx + z \tag{11}$$

$$W_{ZF} = (H^H H)^{-1} H^H \tag{12}$$

$$\hat{x} = W_{ZF}y$$
$$= x + (H^H H)^{-1} H^H z \tag{13}$$
$$= x + \hat{z}$$

Where W_{ZF} is the weighted matrix of the ZF algorithm. $\hat{x}$ is the signal of the detected transmitting antenna and $\hat{z}$ is the noise after detection, $\hat{z} = (H^H H)^{-1} H^H z$. The purpose of the ZF algorithm is to minimize noise power expectations, that is:

$$E\{||\hat{z}||_2^2\} = E\{||(H^H H)^{-1} H^H z||^2\} \tag{14}$$

3.3.2 MMSE algorithm and optimized MMSE algorithm

The MMSE criterion minimizes the expected mean square error (MSE) value between the linear combination of the transmitted signal and the received signal [32–34]. The MMSE algorithm can obtain the optimal

signal-to-interference-plus-noise ratio. The MSE of the channel frequency impulse response between the receiver and the transmitter is:

$$\epsilon = \min E\{|H - \hat{H}|^2\} \tag{15}$$

Where $\hat{H}$ is the minimum estimated value of the channel matrix H under the MMSE algorithm. Both $\hat{H}$ and H are M*1 matrices, and M is the number of signals. When Eq. (15) takes the minimum value, the expression of $\hat{H}$ is:

$$\hat{H} = R_{Hy}R_{yy}^{-1}y \tag{16}$$

$$\begin{aligned} R_{yy} &= E\{yy^H\} \\ &= xR_{HH}x^H + w^2(xx^H)^{-1} \end{aligned} \tag{17}$$

$$R_{Hy} = E\{Hy^H\} = R_{HH}x^H \tag{18}$$

Where x is the input signal, y is the demodulated signal at the receiver, R_{yy} represents the self-covariance matrix of the receiving signal, R_{Hy} represents the cross-covariance matrix of the channel transport function and the receiving signal, R_{HH} is the self-covariance matrix of the channel transport function, and w^2 is the noise variance. $E(.)$ is mathematical expectation, $(.)^H$ is the Hermitian transpose.

This is a typical form of the MMSE channel detection algorithm; the description of optimized MMSE follows is describes as follows.

The minimum error between the demodulated signal value y at the receiver and the output signal y' after channel estimation obtained by the least-square algorithm is:

$$e = \min\{(y - y')^H(y - y')\} \tag{19}$$

$$y' = xH' = xFh' \tag{20}$$

where F is the Fourier transform. Therefore, the Eq. (19) takes a partial derivative of h', and expressed as follows:

$$\begin{aligned} \frac{\partial e}{\partial h'} &= \frac{\partial\{(y - xFh')^H(y - xFh')\}}{\partial h'} \\ &= -2F^H x^H y + 2F^H x^H xFh' \\ &= 0 \end{aligned} \tag{21}$$

$$h' = F^{-1}x^{-1}y \tag{22}$$

$$H' = Fh' = x^{-1}y \tag{23}$$

where the H' is also an M*1 matrix. According to Eqs. (17, 18, 23), Eq.(16) can be converted into:

$$\hat{H} = R_{HH}(R_{HH} + w^2(xx^H)^{-1})^{-1}H' \tag{24}$$

In order to simplify, $(xx^H)^{-1}$ is replaced by $E\{(xx^H)^{-1}\}$ in Eq. (24). When each channel uses the same symbol mapping method and the probability of all symbols appearing at each point on the constellation diagram is the same, there are:

$$E(xx^H)^{-1} = E\{|1/x|^2\} \cdot I \tag{25}$$

$$SNR = E\{|x|^2/w^2\} \tag{26}$$

where I is the identity matrix, and according to Eqs. (25 and 26), Eq. (24) can be converted to:

$$\hat{H} = R_{HH}(R_{HH} + \frac{\beta}{SNR}I)^{-1}H' \tag{27}$$

where $\beta = E\{|x|^2\}E\{|1/x|^2\}$. When different modulation methods are used to modulate the baseband signal, the value of β is also different. If 16QAM modulation is used, $\beta = 17/9$, and QPSK modulation is used in this paper, $\beta = 1$.

Since the above expression also needs to calculate the second-order matrix of the channel and noise, the computational complexity of the above equations is still very high, therefore the channel matrix property can be used, that is, replace the unknown matrix R_{HH} with a matrix whose elements are known at the receiver, thereby avoiding the prior knowledge of the unknown matrix and reducing the computation.

Equation (27) can be expressed as:

$$\hat{H} = R_{HH}^o(R_{HH}^o + \frac{\beta}{SNR} \cdot I)^{-1}H' \tag{28}$$

where R_{HH}^o is a known low-order Hermitian matrix, the eigenvalue is constant, and the elements at the pth row, the qth column are:

$$(R_{HH}^o)_{p,q} = \frac{1 - e^{-2j\pi L(p-q)/M}}{2j\pi L(p-q)/M} \tag{29}$$

where $1 \leq p \leq M$, $1 \leq q \leq M$, L is the number of constant eigenvectors, and R_{HH}^o can be diagonalized in the orthonormal basis, that is:

$$R_{HH}^o = U\Delta U^H \tag{30}$$

where the diagonal elements of Δ are α_i, $1 \leq i \leq M$.

$$\alpha_i = \begin{cases} \frac{1}{L}, 0 \leq i \leq L - 1 \\ 0, L \leq i \leq M - 1 \end{cases} \tag{31}$$

Meanwhile, $R_{HH}^o(R_{HH}^o + \frac{\beta}{SNR} \cdot I)^{-1}$ can be diagonalized in the same way, so Eq. (28) can be transformed into:

$$\hat{H} = U\Delta'U^H H' \tag{32}$$

where Δ' is the eigen decomposition of $R^o_{HH}(R^o_{HH} + \frac{\beta}{SNR} \cdot I)^{-1}$ with diagonal entries α'_i.

$$\alpha'_i = \begin{cases} \frac{\alpha_i}{\alpha_i + \frac{\beta}{SNR}}, & 0 \le i \le L-1 \\ 0 \quad, & L \le i \le M-1 \end{cases} \tag{33}$$

4 Simulation experiment

In the simulation experiment, the Alamouti code is employed, which modulates the high-speed information flow from the source into a low-speed subdata stream and then transmits the low-speed subdata stream via numerous transmitting antennas. QPSK modulates the symbols transmitted by the system. The parameters of modulation are shown in Table 2.

Figure 5a epicts a scatter diagram of the signal modulated by OFDM technology. In contrast, Fig. 5b and c illustrate constellations of the signal at the receiver with 25 dB SNR and 30 dB SNR, respectively. When the received signal is affected by fading and Gaussian noise during transmission, distortion and transmission errors will occur. Figure 5c has a more concentrated signal than Fig. 5b, namely, the signal in Fig. 5b is more distorted, and the transmitted signal has a significantly increased BER.

Figure 6 describes the amplitude of a single OFDM symbol in three cases: the original OFDM symbol, the OFDM symbol with windows, and the OFDM symbol with CP and CS. It can be seen that adding windows to OFDM symbols and adding CP/CS both reduce the effect of multipath interference and eliminate

Parameter	Value
Simulation times	20000
Subcarrier number	512
Effective subcarrier number	200
SNR	20 [dB]
SNR interval	0:2:20 [dB]
CP length	128 [μs]
CS length	30 [μs]
Transmitting antennas number	2
Receiving antennas number	2
Each frame length	10 [fps]
Frames number	10000
Raised cosine window coefficient	3/64
Modulation mode	QPSK

Table 2 Modulation parameters

(a) Scatter plot
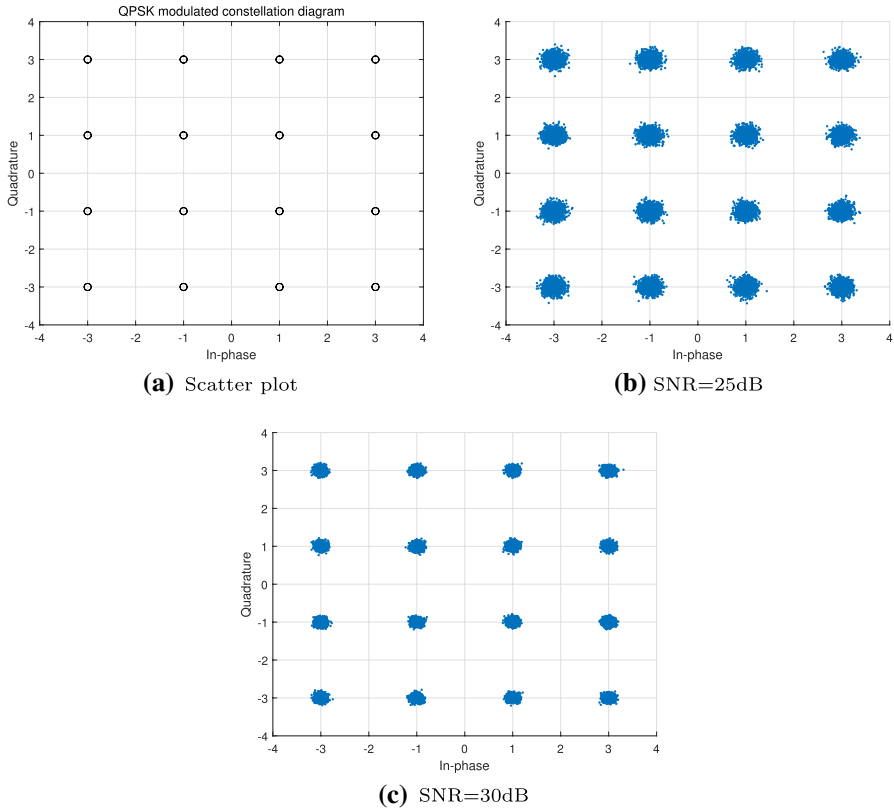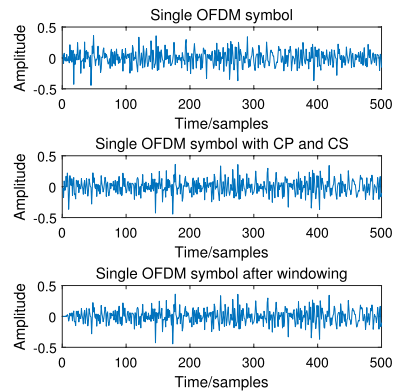
(b) SNR=25dB

(c) SNR=30dB

Fig. 5 Constellation diagram of the signal at the receiver under different SNRs

Fig. 6 OFDM symbol amplitude diagram under different conditions

intercoder interference during transmission. Figure 7a depicts the simulated comparison of OFDM signals under a single-path channel and OFDM signals under a multipath channel. As illustrated in Fig. 7a, the surrounding environment makes the signal reflect, refract, diffuse, and scatter under the multipath channel. In this
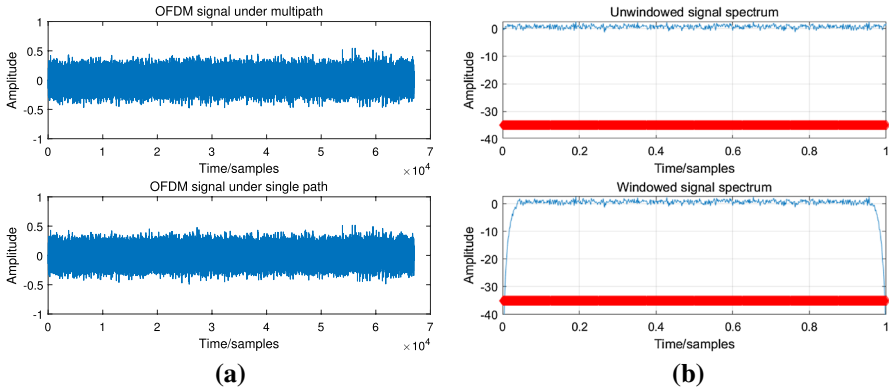
Fig. 7 Simulation diagram of OFDM symbols with different processing

case, the phase difference of different signal paths is complex, which may cause gain or loss to the receiving signal strength. Figure 7b shows a spectrum simulation comparison of an OFDM signal without a window and an OFDM signal with a window. It shows that the spectrum curve of the signal has become smoother, and the spectrum leakage has been reduced after window processing. From the filter point of view, the addition of windows is an additional layer of filter processing, reducing spectrum leakage.

Figure 8a illustrates a capacity simulation of VLC-based MIMO-OFDM systems under known CSI and unknown CSI. As shown in the diagram, when the SNR is the same, the capacity of available CSI systems is always more significant than that of unknown CSI systems. The high reliability of known CSI protects high-speed communication. However, this difference is only noticeable when the SNR is small and when the SNR is close to 20 dB, which has a minimal effect. Figure 8b shows a capacity change diagram when the SNR is 10 dB. When SNR
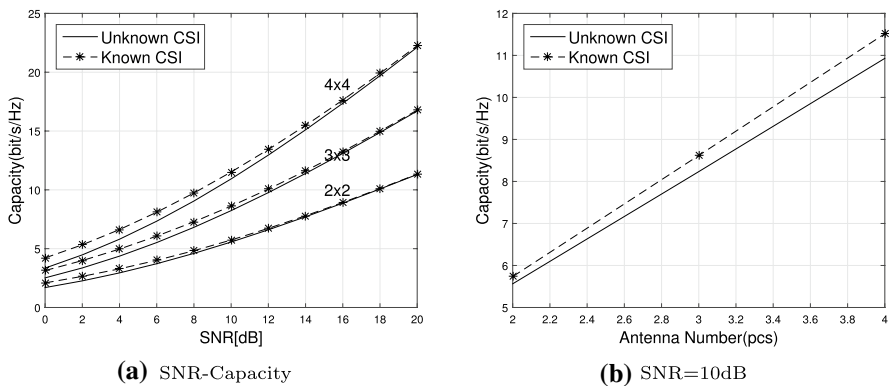

Fig. 8 Relationship between MIMO-OFDM system capacity and SNR and antenna number

is a particular value, the system capacity increases linearly with the increase of the transceiver antenna.

Figure 9 illustrates a performance curve diagram of different numbers of transceivers under the Rayleigh fading channel, which are 1-transmit and 1-receive (that is, single input and single output, SISO), 2-transmit and 1-receive, and 2-transmit and 2-receive systems. Figure 9a and b describe the comparison charts of the SNR-Capacity and SNR-BER curves. It can be seen from the two figures that when the number of LEDs on the transmitter is the same, the more the number of PDs on the receiver, the better the system performance. Similarly, when the number of PDs is the same, the greater the number of LEDs, the better the system performance due to the diversity gain brought by MIMO space-time coding. It can be seen from the comparison of the system performance of 2-transmit 1-receiver and 2-transmit 2-receiver that the effect of adding the receiver is more significant than the effect of adding LED lights. Giving the power combining gain at the receiving end significantly influences transmitter coding because it improves the LEDs' gain.

Figure 10a, b and c illustrate the performance of VLC system using ZF algorithm, MMSE algorithm, and optimized MMSE algorithm under V-BLAST architecture, respectively. The simulation results show the BER performance of the two detection algorithms under three conditions: no interference cancellation, non-ideal interference cancellation, and ideal interference cancellation. The system's performance can be enhanced by eliminating the disturbance, as indicated by the slope of the curve in Fig. 10. Due to the non-ideal interference cancellation using the real-time demodulation effect, the non-ideal disturbance's performance is significantly worse than that of the great disturbance when it is eliminated. The demodulation findings are incorrect, resulting in a significant performance loss.

Figure 11 depicts three different detection algorithms' system performance (BER curve) under ideal and non-ideal interference cancellation conditions. The algorithms all select 4-layer antennas for simulation. As shown in Fig. 11, in the case of non-ideal interference cancellation, real-time demodulation cannot correct all errors; the signal after detection and processing still exists, and the BER
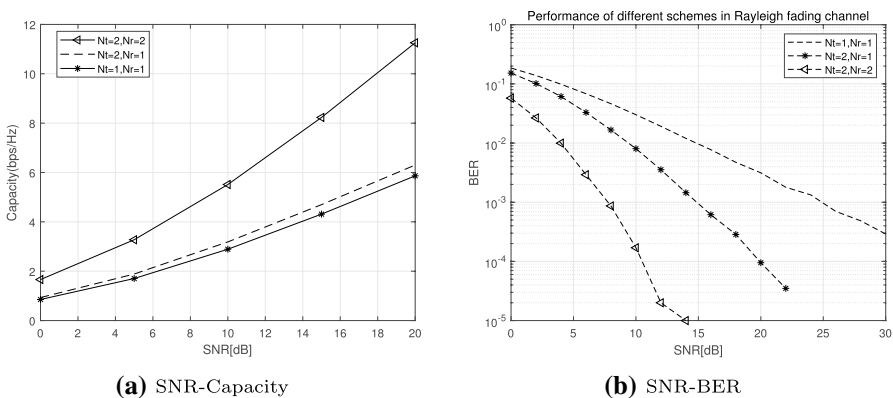

(a) SNR-Capacity   **(b)** SNR-BER

Fig. 9 Performance of different schemes under the Rayleigh fading

(a) V-BLAST-ZF

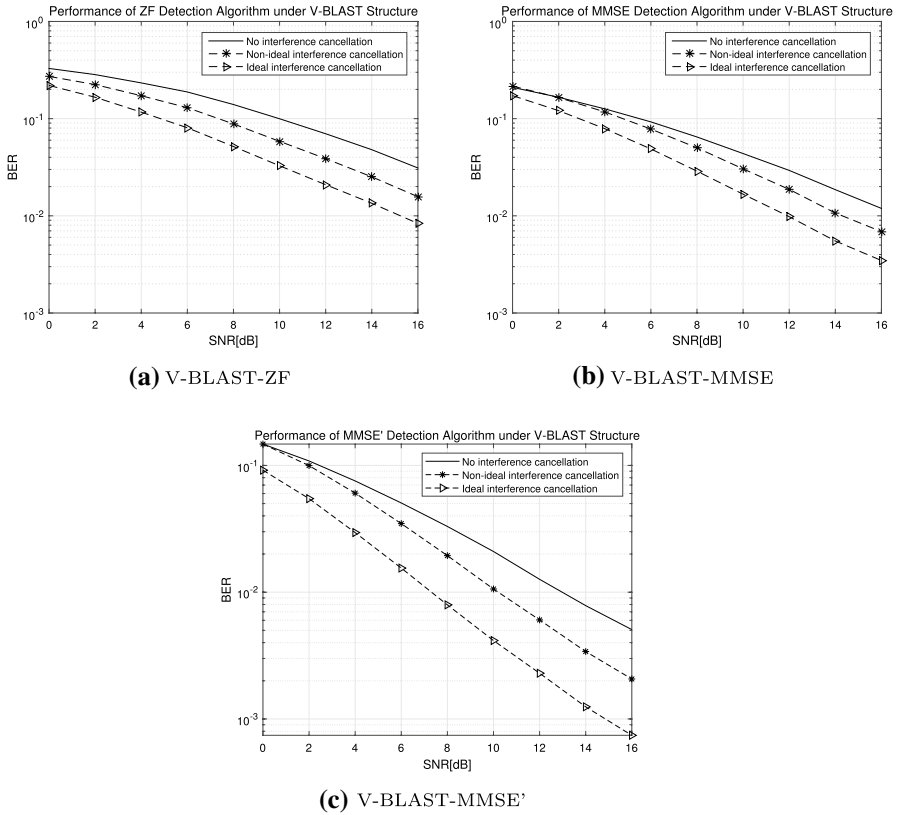**(b)** V-BLAST-MMSE

(c) V-BLAST-MMSE'

Fig. 10 Performance of different detection algorithms under V-BLAST architecture

is high. However, real-time demodulation is used to correct errors in the transmitted data. Meanwhile, in the two cases of ideal interference cancellation and non-ideal interference cancellation, when the SNR is the same, the BER of each layer of the system decreases with the increase of layers. The diversity degree of each detection layer gradually increases, and the diversity degree of the 1st, 2nd, 3rd, and 4th layers is 4, 3, 2, and 1, respectively. The reliability of the layer detected first is the lowest among all layers, and the reliability of the layer detected last is the highest. Secondly, it can be seen from Fig. 11e and f that the optimized MMSE detection algorithm has better BER performance than the other two algorithms under ideal interference conditions.

Figure 12 shows the MSE curves for different algorithms. The channel estimation accuracy of the optimized MMSE algorithm is greater than that of the conventional MMSE algorithm, which will directly impact the system's performance. Figure 13 illustrates a comparison chart of the BER of the three detection algorithms under the VLC-based MIMO-OFDM system. Table 3 shows the data comparison of the BER of the ZF algorithm, the MMSE algorithm, and the optimized
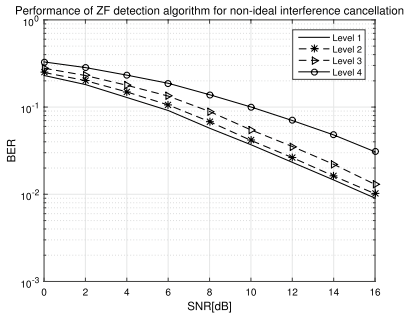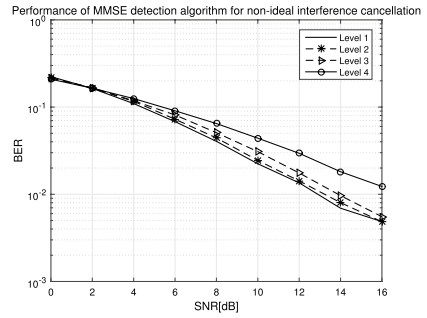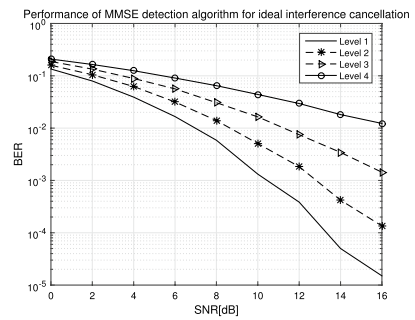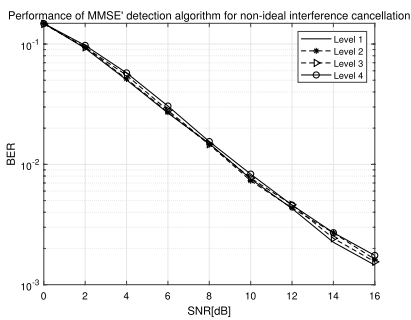
Fig. 11 Performance of different algorithms under different interference cancellations
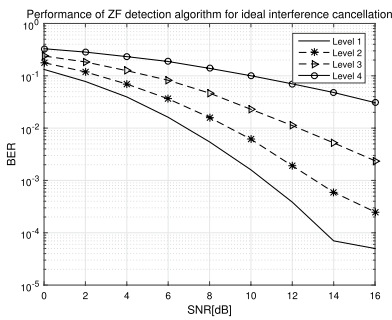
MMSE algorithm. depicted in Fig. 13, the ZF algorithm has the worst performance, followed by the MMSE algorithm, and the optimized MMSE algorithm has the best performance because the optimized MMSE algorithm uses relatively accurate channel statistics. When SNR equals 20 dB, the BER can reach even less than 10^{-4}. When the BER is 10^{-3}, the optimized MMSE algorithm gains 1 dB compared with the conventional MMSE algorithm.
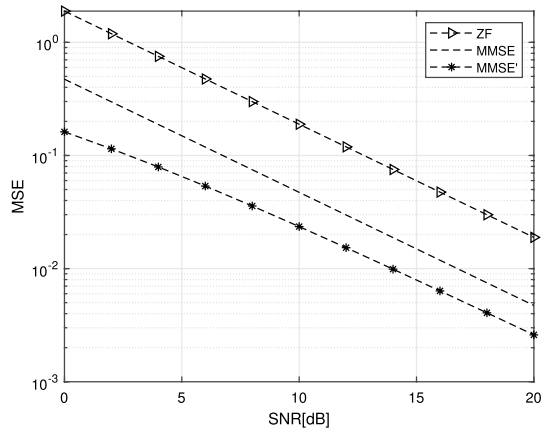
Fig. 12 The MSE curves of different algorithms
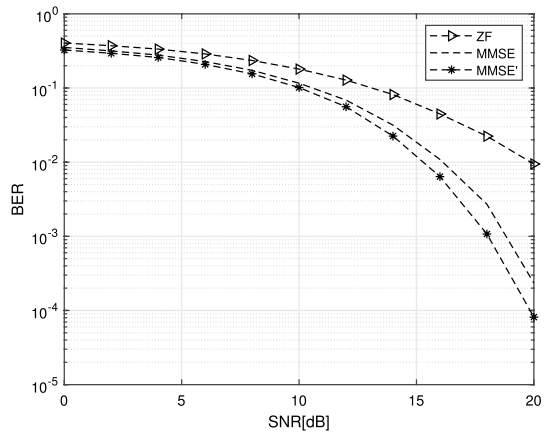

Fig. 13 The BER curves of different algorithms

Table 3 BER of different algorithms

SNR	ZF	MMSE	MMSE'
18 dB	$2.28E-02$	$2.49E-03$	$8.56E-04$
20 dB	$9.26E-03$	$2.47E-04$	$7.81E-05$

5 Conclusion

This paper proposes a MIMO-OFDM system based on VLC that combines MIMO and OFDM technologies to assess system performance in terms of capacity and BER. The proposed system uses OFDM technology to modulate the signal by adding CPs and CSS to the OFDM signal to ensure orthogonality between subcarriers and reduce the interference between symbols and channels caused by multipath interference. Furthermore, the system employs MIMO technology to improve system capacity and enhance the communication quality.

Finally, the performance of the ZF algorithm, the MMSE algorithm, and the optimized MMSE algorithm under ideal interference and non-ideal interference, and the BER of the system under various detection algorithms, are evaluated. This research reveals that the optimized MMSE algorithm has low computational complexity and greater channel estimate accuracy than earlier algorithms, decreasing the system's BER and improving overall performance.

Appendix A: List of acronyms

Acronyms	English Spelling
VLC	Visible Light Communication
LED	Light Emitting Diode
RF	Radio Frequency
OFDM	Orthogonal Frequency Division Multiplexing
MIMO	Multiple Input Multiple Output
SISO	Single Input Single Output
NOHO	Non-Orthogonal Hybrid Optical
SNR	Signal-to-Noise Ratio
FFT	Fast Fourier Transform
IFFT	Inverse Fast Fourier Transform
BER	Bit Error Rate
PD	Photoelectric Detector
AP	Access Point
SDM	Space Division Multiplexing
ISI	Inter-Symbol Interference
ICI	Inter-Channel Interference
CSI	Channel Status Information
CP	Cyclic Prefix
CS	Cyclic Suffix
V-BLAST	Vertical Bell laboratories layered space-time
ZF	Zero Forcing
ZF-SIC	Zero Forcin Successive Interface Cancellation
MMSE	Minimum Mean Square Error
MMSE-SIC	Minimum Mean Square Error Successive Interface Cancellation
ISIC	Iterative Successive Interface Cancellation
QPSK	Quadrature Phase Shift Keying

Data availability Some or all data, models, or code generated or used during the study are available in a repository or online in accordance with funder data retention policies (Provide full citations that include URLs or DOIs.)

Declarations

Conflict of interest We declare that we have no conflict of interest.

References

1. Khan LU (2017) Visible light communication: applications, architecture, standardization and research challenges. Dig Commun Netw 3(2):78–88
2. Li Huai, Minjuan Zhang, Qing Lin (2020) Indoor communication method based on white-light LED. Foreign Electron Meas Technol 39(6):13–17
3. Sun-Young Jung, Do-Hoon Kwon, Se-Hoon Yang, Sang-Kook Han (2016) Inter-cell interference mitigation in multi-cellular visible light communications. Opt Express 24(8):8512–8526
4. Xizheng Ke, Huan Zhang (2018) Indoor visible light uplink communication system based on inverse modulation. Laser Optoelectron Prog 55(2):115–122
5. Xizheng Ke, Yan Lei, Ying Zhang (2019) Research on OFDM system based on Hartley transform in visible light communication. J Sig Process 35(2):266–274
6. Gismalla MSM, Abdullah MFL, Das B, Mabrouk Wafi A, Mahfouz Nouran E (2019) Design of an optical attocells configuration for an indoor visible light communications system. AEUE-Int J Electron Commun 112:152946
7. Zhong Weizhi Su, Sheng Liu Xin, Qingfeng Jing (2017) Improved channel estimation algorithm based on cyclic prefix for MIMO-OFDM. Sys Eng Electron 39(1):188–192
8. Peng Xishun Lu, Anjiang Jia Mingjun, Xuemin Lu (2022) Research on noise reduction of indoor visible light communication based on MIMO-OFDM. J Northeast Univ (Nat Sci) 43(2):176–182
9. Yongsheng Xie, Leilei Zhou, Jianpo Liu (2018) Linearly time-varying channel estimation method with ICI mitigation for OFDM systems. Inf Technol 1:67–70
10. Dong Yang, Xinji Tian (2016) Interference cancellation method based on space-time code for MIMO interference channel. J China Univ Posts Telecommun 23(3):45–50
11. Yiheng Zhao, Peng Zou, Meng Shi, Nan Chi (2019) Nonlinear predistortion scheme based on Gaussian kernel-aided deep neural networks channel estimator for visible light communication system. Opt Eng 58(11):116108. https://doi.org/10.1117/1.OE.58.11.116108
12. Li Chen, Weidong Wang, Chi Zhang (2017) Coalition formation for interference management in visible light communication networks. IEEE Transact Veh Technol 66(8):7278–7285
13. Haoran S, Xiangyi C, Qingjiang S, Hong M, Fu X, Sidiropoulos ND (2018) Learning to optimize: training deep neural networks for interference management. IEEE Transact Sig Process 66(20):5438–5453
14. Jha MK, Kumar N, Lakshmi YVS (2020) NOMA MIMO visible light communication with ZF-SIC and MMSE-SIC, 2020 2nd Ph.D colloquium on ethically driven innovation and technology for society, Ph.D EDITS, pp 1-2, https://doi.org/10.1109/PhDEDITS51180.2020.9315316
15. Anusree A, Jeyachitra R. K. (2016) Performance analysis of a MIMO VLC (visible light communication) using different equalizers. In: 2016 International Conference on Wireless Communications, Signal Processing and Networking (WiSPNET). pp 43-46
16. Xuan Huang, Fang Yang, Changyong Pan, Jian Song (2021) Flexible NOMA-based NOHO-OFDM scheme for visible light communication with iterative interference cancellation. Opt Express 29(4):5645–5657
17. Zhao L, Ng D, Wing K, Yuan J (2017) Multi-user precoding and channel estimation for hybrid millimeter wave systems. IEEE J Sel Areas Commun 7(35): 1576-1590 Khan Lu (2017) Visible light communication: applications, architecture, standardization and research challenges. Dig Commun Netw 3(2):78-88

18. Gao Zhen Hu, Chen Dai Linglong, Zhaocheng Wang (2016) Channel estimation for millimeter-wave massive MIMO with hybrid precoding over frequency-selective fading channels. IEEE Commun Let 6(20):1259–1262
19. Gonzalez-Coma JP, Rodriguez-Fernandez J, Gonzalez-Prelcic N, Castedo L, Heath RW (2018) Channel estimation and hybrid precoding for frequency selective multiuser mmWave MIMO systems. IEEE J Sel Top Sig Process 12(2):353–367
20. Bakulin M, Kreyndelin V, Rog A, Petrov D, Melnik S (2017) Low-complexity iterative MIMO detection based on turbo-MMSE algorithm. Lecture Notes in Computer Science. vol 10531 LNCS, pp 550-560
21. Sahar Said, Waleed Saad, Mona Shokair (2019) MMSE algorithm based two stages hybrid precoding for millimeter wave massive MIMO systems. Analog Integr Circuits Sig Process 98(3):565–573
22. Chen Chen, Wende Zhong, Helin Yang, Sheng Zhang, Pengfei Du (2018) Reduction of SINR fluctuation in indoor multi-cell VLC systems using optimized angle diversity receiver. J Lightwave Technol 36(17):3603–3610
23. Qingqing Hu, Xianqing Jin, Zhengyuan Xu (2018) Compensation of sampling frequency offset with digital interpolation for OFDM-based visible light communication systems. J Lightwave Technol 36(23):5488–5497
24. Chun Du, Fan Zhang, Shuai Ma, Yixiao Tang, Hang Li, Hongmei Wang, Shiyin Li (2019) Secure transmission for downlink NOMA visible light communication networks. IEEE Access 7:65332–65341
25. Touhami R, Slimani D, Khelil A (2018) Analysis of an OFDM based indoor visible light communication system. In: 2018 International Conference on Communications and Electrical Engineering (ICCEE). https://doi.org/10.1109/CCEE.2018.8634433
26. Liwei Y, Xiangyuan P, Furong Z, Yuanhao J, Xinlai L, Wenjie Z (2021) Interference management for indoor multicell visible light communication networks. In: 2021 31st International Telecommunication Networks and Applications Conference (ITNAC). pp 23-29
27. Jung-Lang Yu, Zhang Biling, Yuan Yipu, Hsu Wei-Ting (2020) Blind channel identification for cyclic-prefixed MIMO-OFDM systems with virtual carriers. China Commun 17(3):101–116
28. Badawi WK, El-Hossary MG, Aly MH (2021) Indoor wavelet OFDM VLC-MIMO system: performance evaluation. Symmetry-Basel 13(2):3603–3610
29. Wang D, Mei Z, Liang J, Liu J ()2021 An improved channel estimation algorithm based on WD-DDA in OFDM System. Mob Inf Syst vol 2021, Paper ID: 6540923, https://doi.org/10.1155/2021/6540923
30. Raviteja P, Phan KT, Hong Y, Viterbo E (2018) Interference cancellation and iterative detection for orthogonal time frequency space modulation. IEEE Transact Wirel Commun 17(10):6501–6515
31. Sindhuja R, Shankar A. R (2019) Performance analysis of LEDs in MIMO-OFDM based VLC indoor communication. In: 2019 3rd International Conference on Trends in Electronics and Informatics (ICOEI). pp 1080-1086
32. Yasuhiro Takano, Markku Juntti, Tad Matsumoto (2016) $\ell 1$ LS and $\ell 2$ MMSE-based hybrid channel estimation for intermittent wireless connections. IEEE Transact Wirel Commun 15(1):314–328
33. Dikhaminjia N, He J, Deng H, Tsiklauri M, Drewniak J, Chada A, Mutnury B (2017) Improved MMSE algorithm for DFE optimization. In: IEEE International Symposium on Electromagnetic Compatibility. vol 0, pp 433-436
34. Li M, Li X, Yang C, Yang Q, Yu S (2017) Experimental demonstration of indoor interfered visible light communication system employing successive interference cancellation. Chin Opt Lett 15(5):050604. https://doi.org/10.3788/COL201715.050604

Authors and Affiliations

Liwei Yang[1] [iD] **· Furong Zhu[1] · Wencong Lai[1] · Qiulian Zhang[1] · Xinlai Liu[1] ·
Wenjie Zhang[2]**

Furong Zhu
1070556129@qq.com

Wencong Lai
2437897415@qq.com

Qiulian Zhang
3062441679@qq.com

Xinlai Liu
643844151@qq.com

Wenjie Zhang
Zhan0300@ntu.edu.sg

[1] College of Information and Electrical Engineering, China Agricultural University, Beijing 100083, China

[2] Minnan Normal University, Zhangzhou 363000, Fujian, China